

Supporting Information

Enrichment of Phosphorylated Peptides with Metal-Organic Framework Nanosheets for Serum Profiling of Diabetes and Phosphoproteomics Analysis

Shi-Shu Yang¹, Yu-Jie Chang¹, Hao Zhang², Xizhong Yu², Wenbin Shang², Gui-Quan Chen³, David Da Yong Chen^{1,4,*} and Zhi-Yuan Gu^{1,*}

¹Jiangsu Key Laboratory of Biofunctional Materials, Jiangsu Collaborative Innovation Center of Biomedical Functional Materials, College of Chemistry and Materials Science, Nanjing Normal University, Nanjing 210023, China

²Key Laboratory for Metabolic Diseases in Chinese Medicine, First College of Clinical Medicine, Nanjing University of Chinese Medicine, Nanjing 210023, China

³State Key Laboratory of Pharmaceutical Biotechnology, MOE Key Laboratory of Model Animal for Disease Study, Model Animal Research Center, Nanjing University, 12 Xuefu Avenue, Nanjing, 210061, China

⁴Department of Chemistry, University of British Columbia, Vancouver, BC, Canada, V6T 1Z1

**To whom correspondence should be addressed. E-mail: chen@chem.ubc.ca; guzhiyuan@njnu.edu.cn.*

The synthesized procedure of Ti-based MOF nanosheets, Zr-BTB nanosheets, MIL-125, NH₂-MIL-125.

Ti-based MOF nanosheets.^(S1, S2) H₄DOBDC (0.95 g, 5 mmol) and DEF (3 mL) were mixed in a Teflon lined Paar autoclave of 25 mL. The mixture was stirred at room temperature and 0.35 mL of titanium isopropoxide (1.16 mmol) were added. The reactor was sealed and heated at 200 °C for 20 h (heating rate: 170 °C h⁻¹). Then the mixture was naturally cooled down to room temperature. Finally, the resulting dark solid was repeatedly washed with DEF and dried at room temperature. The Ti-based MOF nanosheets were obtained via a top-down liquid ultrasonication exfoliation method. The dried powders of Ti-based MOF (10 mg) were added to isopropanol (10 mL) by ultrasonication for about 2 days at room temperature. Then the suspension was centrifugated at 3000 rpm for 5 min to get the upper-layer colloidal suspension, after that it was centrifugated at 12000 rpm for 20 min to get the Ti-based MOF nanosheets.

Zr-BTB nanosheets.^(S3) ZrCl₄ (10.12 mg, 0.045 mmol) and H₃BTB (12.5 mg, 0.028 mmol) were dissolved in a mixture of HCOOH (1,113 mg), DMF (5 mL) and deionized (DI) water (60 µL) in a pyrex vial of 25 mL. Then the pyrex vial was kept at 120 °C for 48 h. After cooling to room temperature, white precipitates were obtained and washed three times using DMF and twice using methanol respectively. Finally, the solid white samples were calcined overnight in a vacuum oven.

MIL-125.^(S4) In a typical experiment, a solution of titanium isopropoxide (0.6 mL, 2.0 mmol) and H₂BDC (498 mg, 3.0 mmol) were added to a mixture of DMF and methanol ($V_{\text{DMF}}:V_{\text{methanol}} = 9:1$). The above mixture was stirred for 20 min at room temperature and was transferred to a 25 mL Teflon liner and heated at 150 °C for 20 h. After cooling down to room temperature, the resultant suspension was washed with DMF and methanol respectively. Finally, the solid white product was activated under vacuum at 150 °C for 12 h.

NH₂-MIL-125.^(S5) The highly porous NH₂-MIL-125(Ti) nanoparticles was synthesized by a solvothermal route in a methanol-DMF mixed with solvent with NH₂-BDC and titanium isopropoxide as the organic linker and the metal source. In brief, NH₂-BDC (272 mg, 1.5 mmol) was dissolved in methanol and DMF mixed solvent ($V_{\text{methanol}}: V_{\text{DMF}}$

= 1:9). Then, titanium isopropoxide (0.13 mL, 0.4 mmol) was added to the NH₂-BDC solution. After stirring for 20 minutes, the mixture was transferred to a 20 mL Teflon-lined autoclave and placed in an oven at 150 °C for 72 h. After cooling to room temperature, a yellow powder product was obtained and washed three times using DMF and twice using methanol. Finally, the solid yellow samples were calcined overnight in a vacuum oven at 150 °C for 12 h.

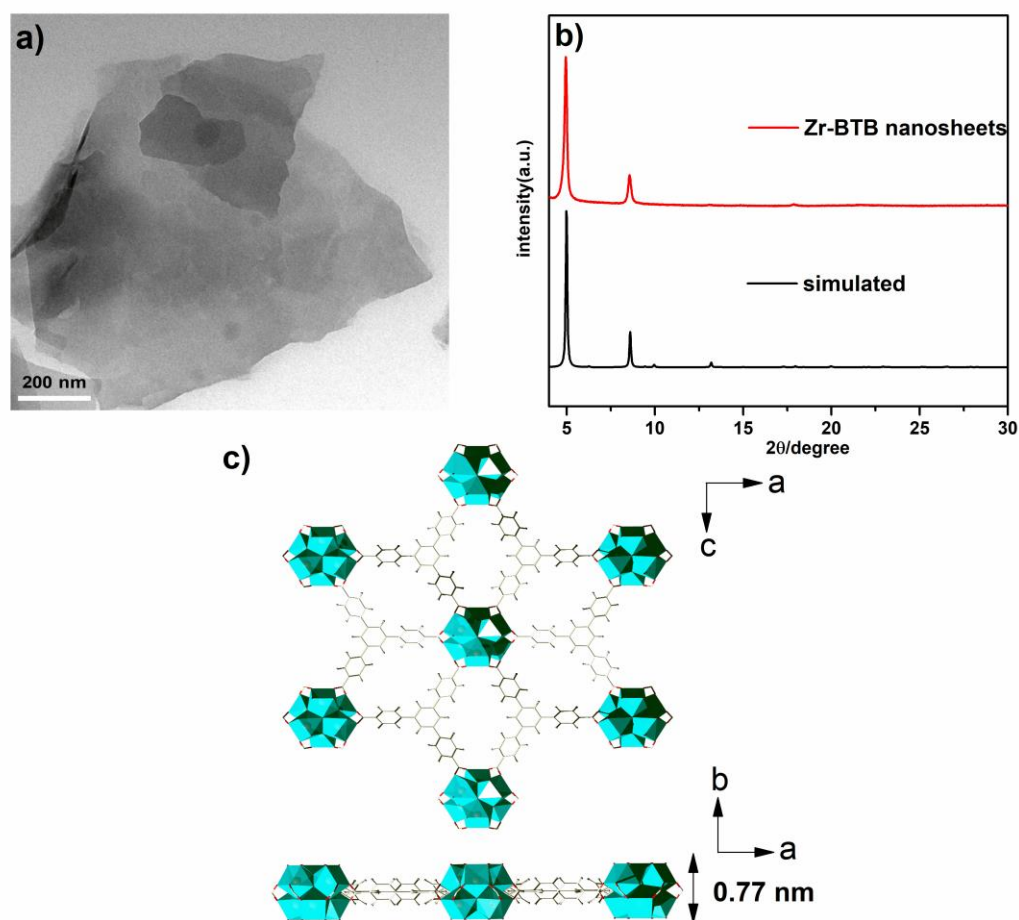


Figure S1. Characterization of Zr-BTB nanosheets. (a) TEM image of Zr-BTB nanosheets. (b) Powder XRD data for simulated Zr-BTB nanosheets (Powder Pattern Settings: Include preferred orientation, $h=0$, $k=1$ and $l=0$, respectively. March-Dollase parameter: 4.5), and Zr-BTB nanosheets. (c) The crystal structure of a single layer of Zr-BTB nanosheet. The Zr, C, and O atoms are shown in orange, grey, and red, respectively.

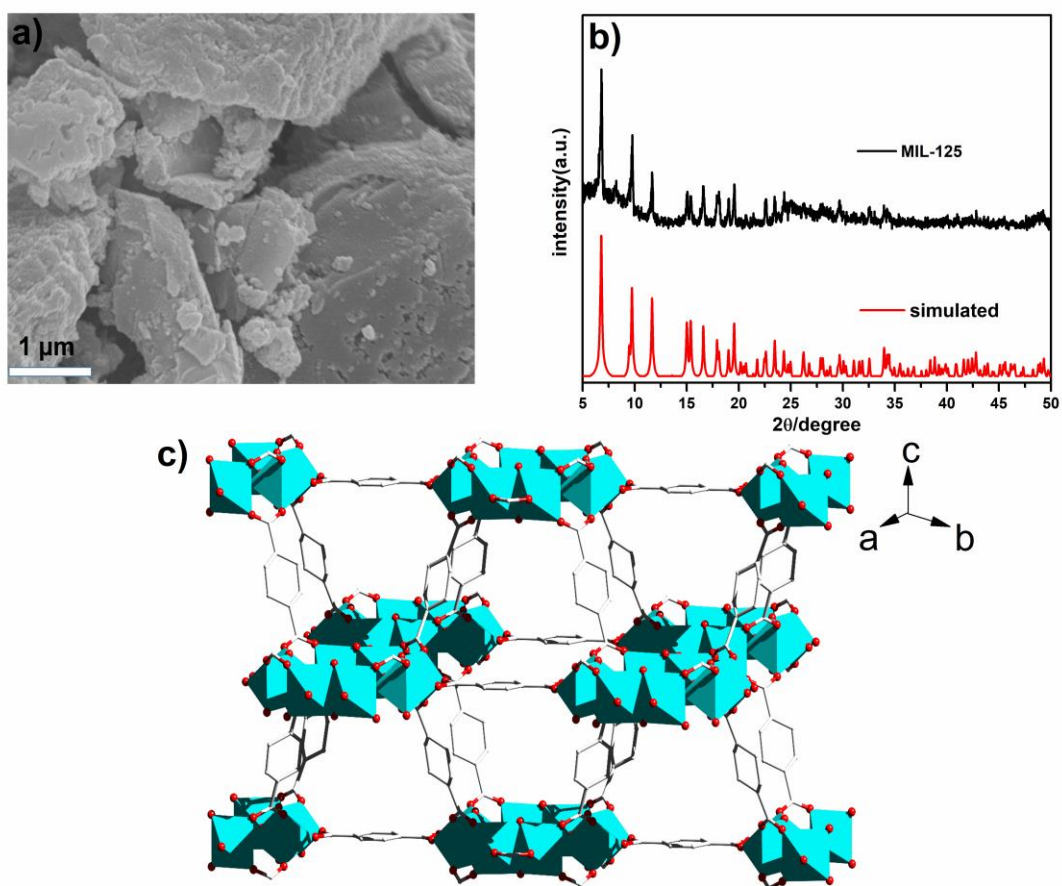


Figure S2. Characterization of MIL-125. (a) SEM image of MIL-125. (b) Powder XRD data for simulated MIL-125, and MIL-125. (c) The crystal structure of MIL-125. The Ti, C, and O atoms are shown in blue, grey, and red, respectively.

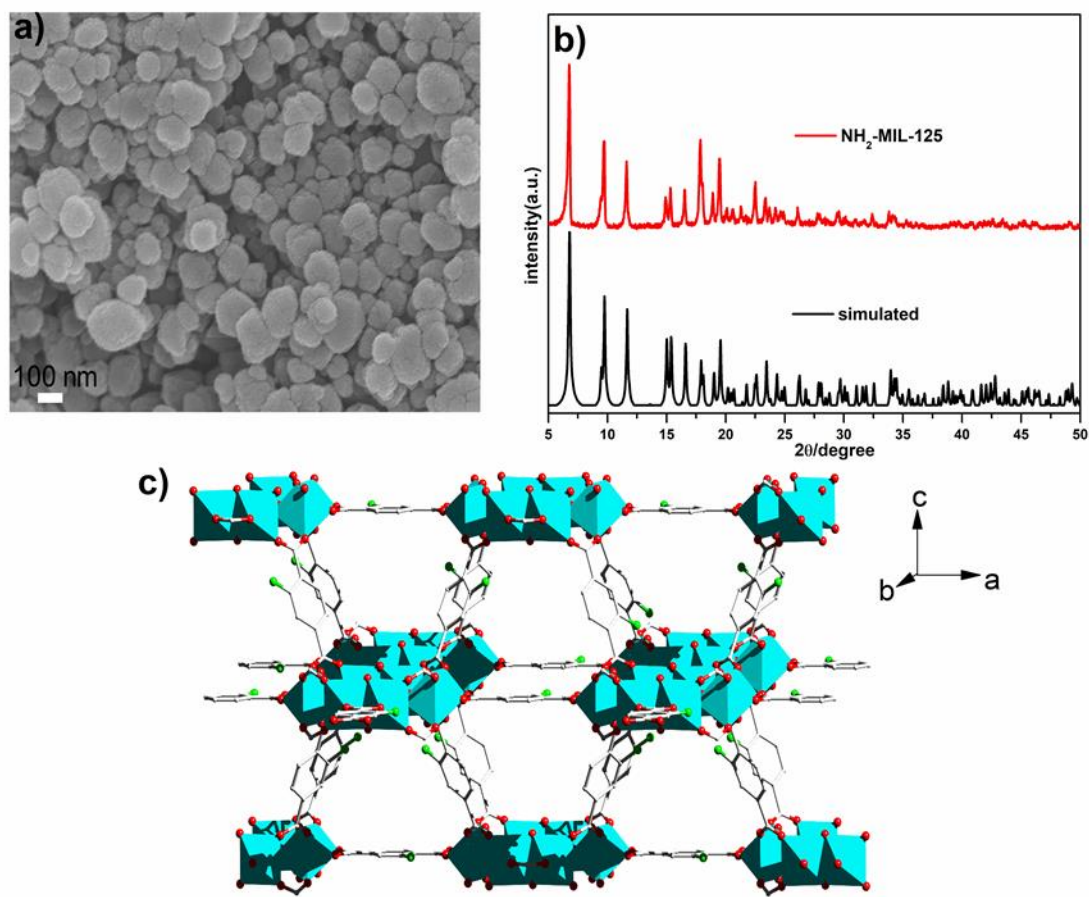


Figure S3. Characterization of $\text{NH}_2\text{-MIL-125}$. (a) SEM image of $\text{NH}_2\text{-MIL-125}$. (b) Powder XRD data for simulated $\text{NH}_2\text{-MIL-125}$ and $\text{NH}_2\text{-MIL-125}$. (c) The crystal structure of $\text{NH}_2\text{-MIL-125}$. The Ti, C, O, and N atoms are shown in blue, grey, red, and green, respectively.

Table S1. Detailed information of detected phosphopeptides enriched from the tryptic digest of α -casein, β -casein and non-fat milk.

Peak No.	m/z	No. of phosphorylation	Peptide sequences
α 1	1237.2	1	TVDMEpSTEVF
α 2	1661.3	1	VPQLEIVPNpSAEER
α 3	1927.2	2	DIGpSEpSTEDQAMEDIK
α 4	1943.5	2	DIGpSEpSTEDQAoMEDIK
α 5	1952.8	1	YKVPQLEIVPNpSAEER
α 6	2618.2	4	NTMEHVpSpSpSEESIIpSQETYSK
α 7	2635.2	4	NToMEHVpSpSpSEESIIpSQETYSK
α 8	2677.8	3	VNELpSKDIGpSEpSTEDQAMEDIK
α 9	2703.5	5	Q*MEAEpSIpSpSpSEEIVPNpSVEQK
α 10	2720.4	5	QMEAEpSIpSpSpSEEIVPNpSVEQK
α 11	2735.9	5	QoMEAEpSIpSpSpSEEIVPNpSVEQK
α 12	2935.6	3	EKVNELpSKDIGpSEpSTEDQAMEDIK
α 13	3007.3	4	NANEEYpSIGpSpSpSEESAEEVATEEVS
α 14	3087.9	5	NANEEYpSIGpSpSpSEEpSAEEVATEEVS
β 1	2061.6	1	FQpSEEQQQTEDELQDK
β 2	2556.4	1	FQpSEEQQQTEDELQDKIHPF
β 3	2965.7	4	ELEELNVPGEIVEpSLpSpSpSEESITR
β 4	3122.1	4	RELEELNVPGEIVEpSLpSpSpSEESITR

Q*, pyroglutamylation on the N-terminal Gln.

Ao, To, Qo, oxidation on methionine.

Table S2. Detailed information of the enrichment efficiency of Ti-based MOF nanosheets from tryptic digests of β -casein that compared to Zr-BTB nanosheets, other two Ti-MOFs (MIL-125 and NH₂-MIL-125) and TiO₂ nanoparticles.

	Ti-based MOF	Zr-BTB	MIL-125	NH ₂ -MIL-	TiO ₂
	nanosheets	nanosheets		125	nanoparticles
β 1	✓	✓	✓	✓	✓
β 2	✓		✓	✓	✓
β 3	✓		✓	✓	✓
β 4	✓		✓	✓	✓
β 4 ²⁺	✓				
nonphosphopeptides		✓	✓	✓	✓
number of detected dephosphorylated peptides	5	nd	3	3	4
NL	4.0E+4	4.0E+3	8.0E+3	1.4E+4	1.4E+4

β 4²⁺ : The tetra-phosphorylated peptide with two units of positive charge.

NL : normalized level.

nd : not detected.

Table S3. The comparison of 2-D Ti-based MOF nanosheets with other MOFs materials in terms of the selectivity and the detection limits.

	2-D Ti-based MOF nanosheets	Zr-BTB nanosheets	MIL-125	NH ₂ -MIL-125
Selectivity	100%	10%	70%	70%
Detection limits (S/N)	0.5 fmol μL^{-1}	2000 fmol μL^{-1}	400 fmol μL^{-1}	20 fmol μL^{-1}

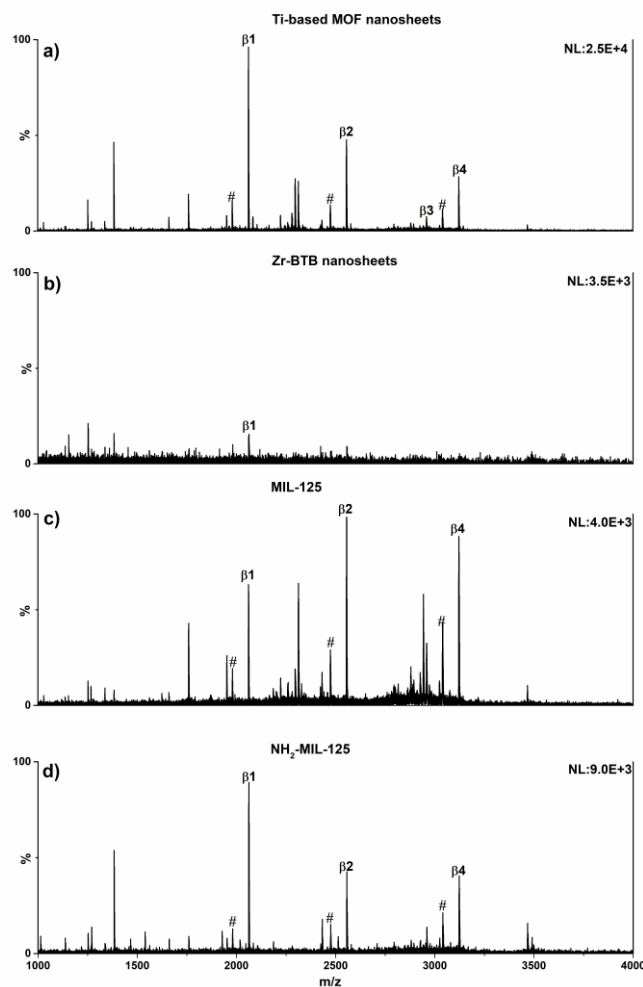


Figure S4. Mass spectrum of phosphopeptides from tryptic digest of β -casein (4×10^{-6} M) enrichment with different materials. (a) Ti-based MOF nanosheets, (b) Zr-BTB nanosheets, (c) MIL-125 and (d) NH_2 -MIL-125 (#: dephosphorylated residue of corresponding peptides (m/z : $[M+H]^+ - 80$); all unmarked peaks are from non-phosphopeptides; $\beta 1$: No. 1 phosphopeptide from β -casein; NL: Normalized Level). The detected phosphopeptides with m/z value and amino acid sequences are listed in Table S1.

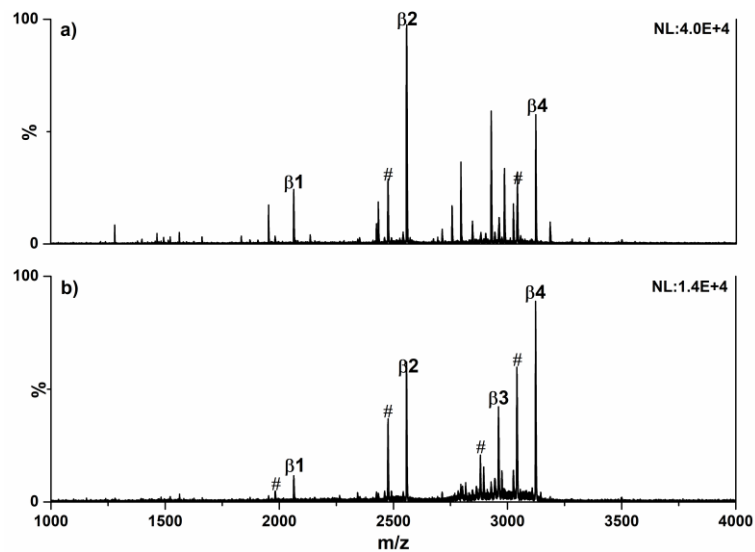


Figure S5. Mass spectrum of phosphopeptides from tryptic digest of β -casein (4×10^{-6} M) enrichment with TiO_2 nanoparticles by different treated process. (a) unpretreated TiO_2 nanoparticles. (b) pretreated by β -glycerophosphate disodium TiO_2 nanoparticles (#: dephosphorylated residue of peptides (m/z : $[M+H]^+ - 80$); all unmarked peaks are from non-phosphopeptides; $\beta 1$: No. 1 phosphopeptide from β -casein; NL: Normalized Level). The detected phosphopeptides with m/z value and amino acid sequences are listed in Table S1.

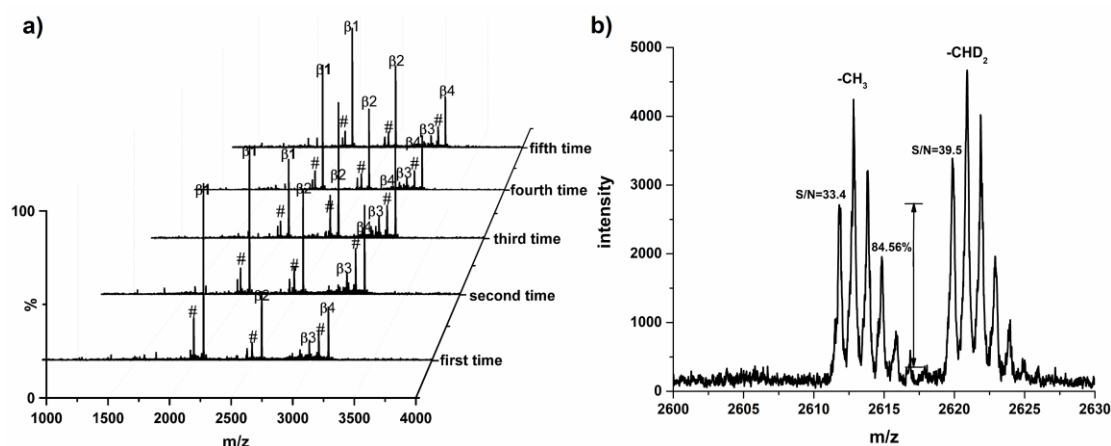


Figure S6. Mass spectrum of phosphopeptides from tryptic digest of β -casein (4×10^{-6} M) enriched with Ti-based MOF nanosheets to show (a) the reproducibility and (b) the recovery. (#: dephosphorylated residue of peptides (m/z : $[M+H]^+ - 80$); all unmarked peaks are from non-phosphopeptides; $\beta 1$: No. 1 phosphopeptide from β -casein; NL: Normalized Level). Recovery was calculated from the measurements of 1:1 mixture of the D-labelled and H-labelled $\beta 2$ peaks.^(S6)

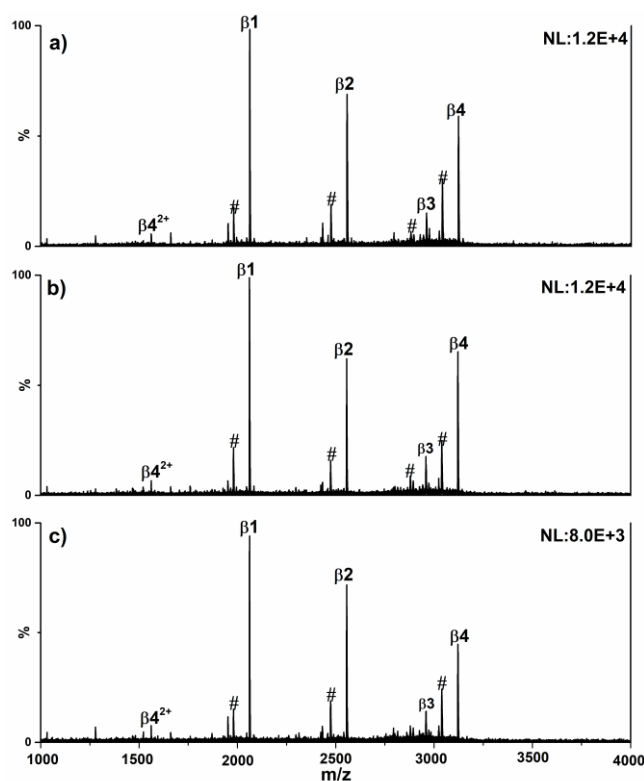


Figure S7. Mass spectra of phosphopeptides from tryptic digest of β -casein (4×10^{-6} M) enriched with Ti-based MOF nanosheets by different pretreated solutions (a) 10 mM β -glycerophosphate disodium. (b) 10 mM NaCl and (c) 10 mM KCl (#: dephosphorylated residue of corresponding peptides (m/z : $[M+H]^+ - 80$); all unmarked peaks are from non-phosphopeptides; $\beta 1$: No. 1 phosphopeptide from β -casein; NL: Normalized Level). The detected phosphopeptides with m/z value and amino acid sequences are listed in Table S1.

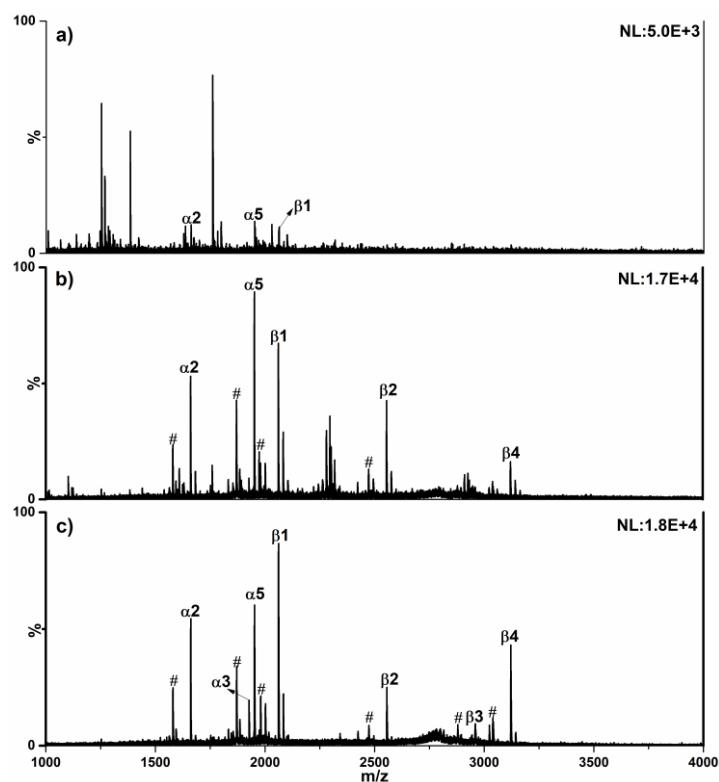


Figure S8. Direct Analysis of tryptic digest of nonfat milk and enrichment with Ti-based MOF nanosheets by different treated process. (a) direct analysis and enrichment with (b) unpretreated Ti-based MOF nanosheets and (c) pretreated by β -glycerophosphate disodium Ti-based MOF nanosheets (#: dephosphorylated residue of peptides (m/z : $[M+H]^+-80$); all unmarked peaks are from non-phosphopeptides; $\beta 1$: No. 1 phosphopeptide from β -casein; NL: Normalized Level). The detected phosphopeptides with m/z value and amino acid sequences are listed in Table S1.

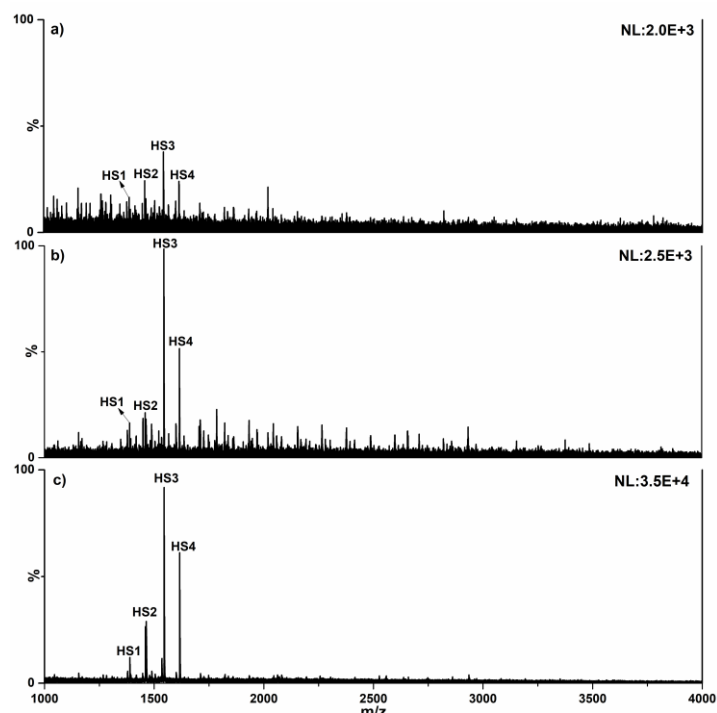


Figure S9. Direct Analysis of human serum and enrichment with Ti-based MOF nanosheets by different treated process. (a) direct analysis and enrichment with (b) unpretreated Ti-based MOF nanosheets and (c) pretreated by β -glycerophosphate disodium Ti-based MOF nanosheets (#: dephosphorylated residue of peptides (m/z : $[M+H]^+-80$); all unmarked peaks are from non-phosphopeptides; $\beta 1$: No. 1 phosphopeptide from β -casein; NL: Normalized Level). The detected phosphopeptides with m/z value and amino acid sequences are listed in Table 1.

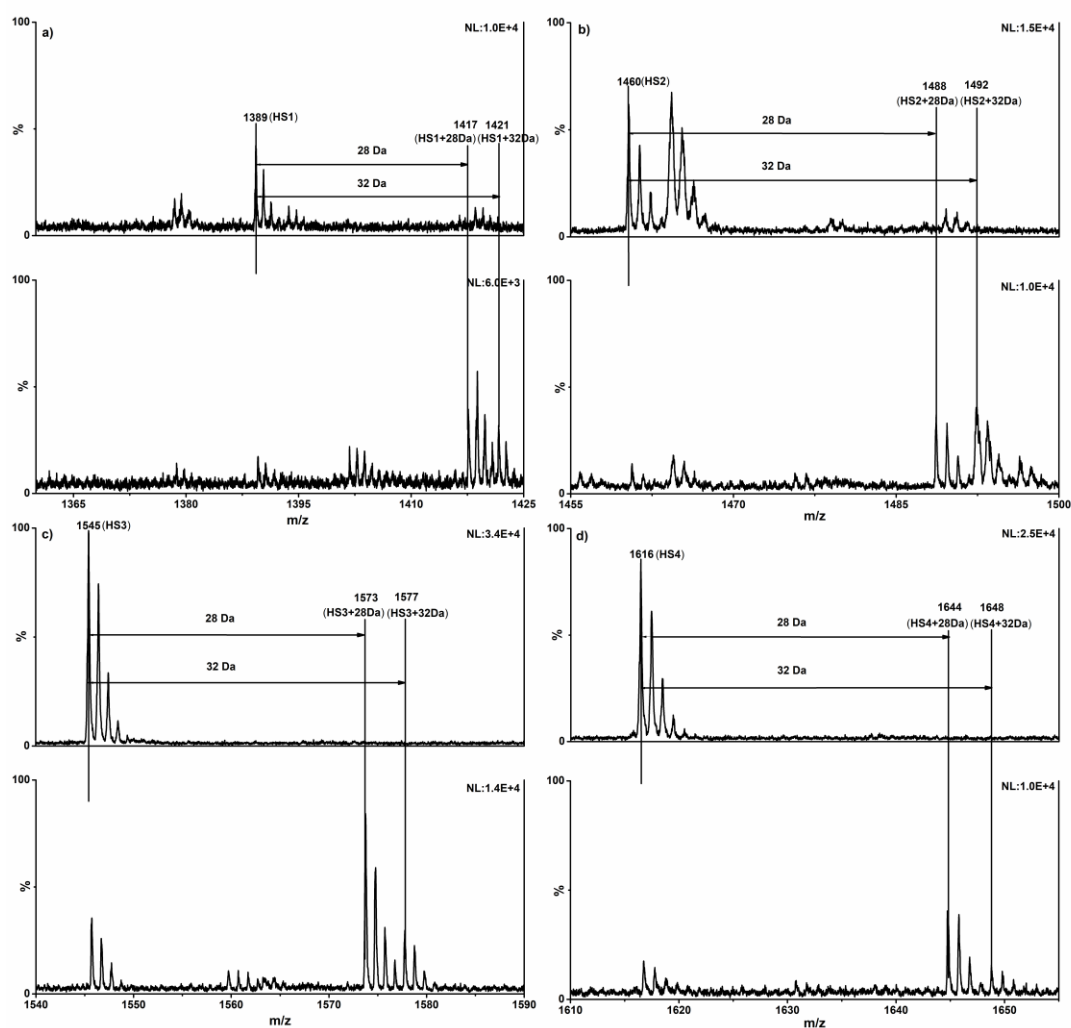


Figure S10. Representative MALDI-TOF MS spectra of FPA from serum phosphopeptides labeled *in situ* by CH₂O and CD₂O, respectively and the labeling reactions are as follows. (a) HS1. (b) HS2. (c) HS3. and (d) HS4.

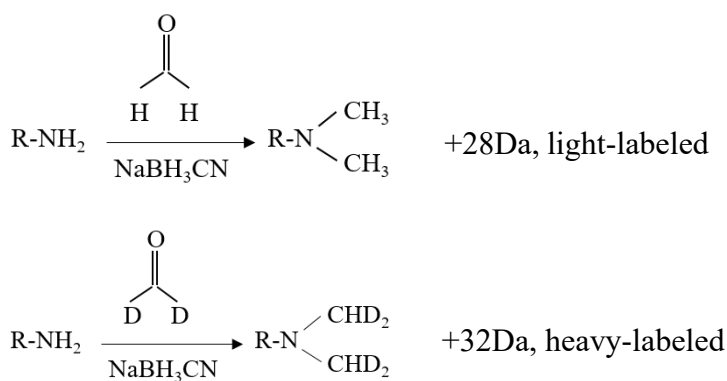


Table S4. Peak area information of endogenous phosphopeptides captured from human serum using 2-D Ti-based MOF nanosheets and labeled by CH₂O (HV1, healthy volunteers) and CD₂O (DP1, diabetes patients) according the *in situ* labeling strategy at different pipette ratio, every peak area was calculated from the isotope peak that labeled by CH₂O and CD₂O, respectively.

NO.	pipette ratio		1:4		1:1		4:1	
	peak area	peak area	peak area	peak area	peak area	peak area	peak area	
HS1	630	2161	3320	8554	1926	3578		
HS2	2902	1013	6225	2947	2203	979		
HS3	468	4531	1771	10427	1120	2799		
HS4	160	1776	227	2076	118	957		

Table S5. Peak area information of endogenous phosphopeptides captured from human serum using 2-D Ti-based MOF nanosheets and labeled by CH₂O (HV2, healthy volunteers) and CD₂O (DP2, diabetes patients) according the *in situ* labeling strategy at different pipette ratio, every peak area was calculated from the isotope peak that labeled by CH₂O and CD₂O, respectively.

NO.	pipette ratio		1:4		1:1		4:1	
	peak area	peak area	peak area	peak area	peak area	peak area	peak area	peak area
HS1	939	2588	1566	2431	3240	3220		
HS2	3859	709	4077	528	4555	482		
HS3	1366	6134	2737	5224	5212	3660		
HS4	497	1838	589	1589	549	1108		

Table S6. Peak area information of endogenous phosphopeptides captured from human serum using 2-D Ti-based MOF nanosheets and labeled by CH₂O (HV3, healthy volunteers) and CD₂O (DP3, diabetes patients) according the *in situ* labeling strategy at different pipette ratio, every peak area was calculated from the isotope peak that labeled by CH₂O and CD₂O, respectively.

NO.	pipette ratio		1:4		1:1		4:1	
	peak area	peak area	peak area	peak area	peak area	peak area	peak area	
HS1	484	4347	1142	3266	389	1870		
HS2	3440	567	2268	583	2620	104		
HS3	1544	4266	4152	4815	1828	5430		
HS4	856	2320	946	1224	1009	662		

Table S7. Detailed information of identified phosphopeptides from mouse brain neocortex lysate by 2-D Ti-based MOF nanosheets. (A separate Excel file)

Table S8. Unique phosphorylation sites information identified from mouse brain neocortex lysate by 2-D Ti-based MOF nanosheets. (A separate Excel file)

Table S9. Detailed information of identified phosphopeptides from mouse spinal cord lysate by 2-D Ti-based MOF nanosheets. (A separate Excel file)

Table S10. Unique phosphorylation sites information identified from mouse spinal cord lysate by 2-D Ti-based MOF nanosheets. (A separate Excel file)

Table S11. Detailed information of identified phosphopeptides from mouse testis lysate by 2-D Ti-based MOF nanosheets. (A separate Excel file)

Table S12. Unique phosphorylation sites information identified from mouse testis lysate by 2-D Ti-based MOF nanosheets. (A separate Excel file)

References

- (S1) H. Xu, J. Gao, X. Qian, J. Wang, H. He, Y. Cui, Y. Yang, Z. Wang, G. Qian, *J. Mater. Chem. A* **2016**, 4, 10900-10905.
- (S2) H. Assi, L. C. Pardo Pérez, G. Mouchaham, F. Ragon, M. Nasalevich, N. Guillou, C. Martineau, H. Chevreau, F. Kapteijn, J. Gascon, P. Fertey, E. Elkaim, C. Serre, T. Devic, *Inorg. Chem.* **2016**, 55, 7192-7199.
- (S3) L. Cao, Z. Lin, F. Peng, W. Wang, R. Huang, C. Wang, J. Yan, J. Liang, Z. Zhang, T. Zhang, L. Long, J. Sun, W. Lin, *Angew. Chem. Int. Ed.* **2016**, 55, 4962-4966.
- (S4) S.-N. Kim, J. Kim, H.-Y. Kim, H.-Y. Cho, W.-S. Ahn, *Catal. Today* **2013**, 204, 85-93.
- (S5) S. Hu, M. Liu, K. Li, Y. Zuo, A. Zhang, C. Song, G. Zhang, X. Guo, *CrystEngComm* **2014**, 16, 9645-9650.
- (S6) Zhao, Y.; Zhang, L.; Chu, Z.; Xiong, Z.; Zhang, W. *Anal. Methods* **2017**, 9, 443-449.